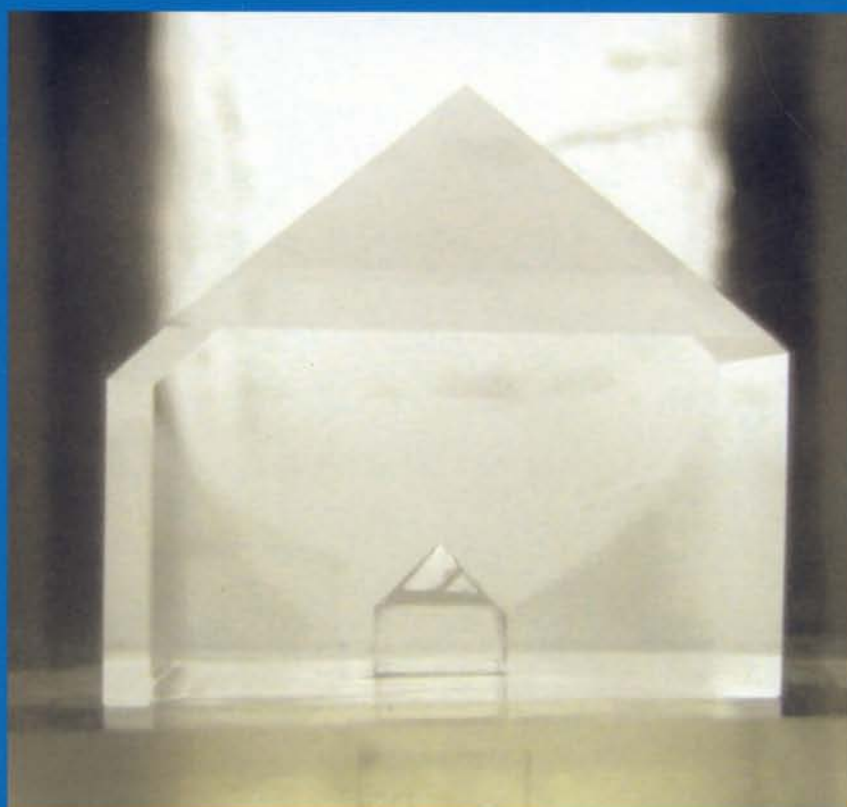
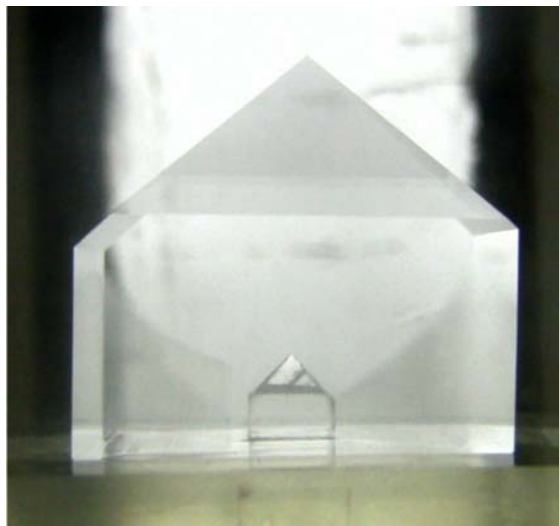


Crystal Research and Technology

Journal of Experimental and Industrial Crystallography



Growth and properties of
Ba-doped KDP crystals
(Guozong Zheng, Genbo Su,
Xinxin Zhuang, Xiuqin Lin,
and Zhengdong Li, p. 811)



COVER PICTURE

The cover picture shows a growing KDP crystal from solution. A Z-cut seed crystal with size of $10 \times 10 \times 5 \text{ mm}^3$ can be seen in the growing crystal. (see pages 811 – 816).

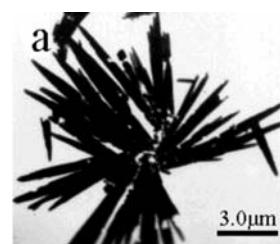
ORIGINAL PAPERS

Page 797–800

Long Chen, Yuhua Shen, Anjian Xie, Fangzhi Huang, Shikuo Li, and Qingfeng Zhang

Synthesis of rhombohedral strontium carbonate aggregates at the water/hexamethylene interface with cetyltrimethylammonium bromide

Unusual rhombohedral strontium carbonate (SrCO_3) aggregates have been synthesized in situ from strontium nitrate by the slow release of carbon dioxide by alkaline hydrolysis of diethyl carbonate at the water/hexamethylene interface in the presence of cetyltrimethylammonium bromide (CTAB). Transmission electron microscopy, Fourier transform infrared spectroscopy and X-ray powder ...



Page 801–805

Taohua Huang, Shengming Zhou, Hao Teng, Hui Lin, and Jun Wang

Growth, etching morphology and spectra of LiAlO_2 crystal

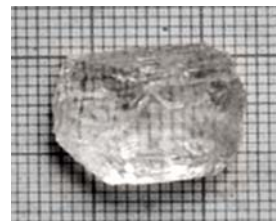
γ - LiAlO_2 single crystal was successfully grown by Czochralski method. The crystal quality was characterized by X-ray rocking curve and chemical etching. The effects of air-annealing and vapor transport equilibration (VTE) on the crystal quality, etch pits and absorption spectra of LiAlO_2 were also ...



Page **806–810** _____ J. Mary Linet, S. Mary Navis Priya, S. Dinakaran, and S. Jerome Das

Dielectric and microhardness studies on L-citrulline and L-ascorbic acid admixture TGS crystals

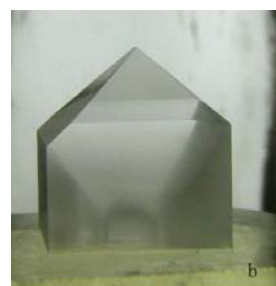
Single crystals of amino acid doped (L-citrulline, L-ascorbic acid) triglycine sulphate were grown by slow evaporation technique. The lattice parameters and crystalline quality were confirmed by powder X-ray diffraction studies. The presence of functional groups in the grown crystals was confirmed by Fourier transform infrared spectrum analysis. The dielectric studies were carried out to identify the phase ...



Page **811–816** _____ Guozong Zheng, Genbo Su, Xinxin Zhuang, Xiuqin Lin, and Zhengdong Li

Growth and properties of Ba-doped KDP crystal

KDP crystals were rapidly grown from solution doped with different Ba^{2+} concentrations. The effects of Ba^{2+} on the growth rate, morphology and quality of KDP crystals were discussed. Significant changes in shapes and volume of the grown crystals have been observed. During the growth process, defect region expands gradually with the increasing Ba^{2+} concentration. Samples were cut from different parts of the as-grown crystals for investigating the optical quality ...



Page **817–822** _____ Guang-Ru Tian, Si-Xiu Sun, Xin-Yu Song, Wei Zhao, and Ting You

Catanionic surfactants assisted synthesis of dilead pentaoxochromate nanorods

Single-crystalline dilead pentaoxochromate (Pb_2CrO_5) with nanorod-shape has been synthesized by adjusting the pH value of the catanionic reverse micelles formed by a cationic surfactant CTAB (hexadecyltrimethylammonium bromide) and an anionic surfactant SDS (sodium dodecyl sulfonate), followed by a hydrothermal process. The results show that ...



Page **823–827** _____ C. Justin Raj, M. B. Lincoln, and S. Jerome Das

Synthesis and characterization of doped lithium aluminate nanocrystalline particles by sol-gel method

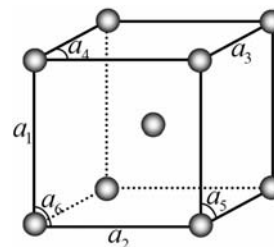
Nanocrystalline particles of Co^{2+} doped lithium aluminate (Co^{2+} :LAO) and Ni^{2+} -doped lithium aluminate (Ni^{2+} :LAO) were synthesized by sol-gel method. The crystalline nature and particle size of the samples were characterized by X-ray diffraction analysis (XRD). The morphology and the presence Co^{2+} and Ni^{2+} in ...



Page 828–836 _____ Jian-Min Zhang, Jing-Zhou Wang, and Ke-Wei Xu

MAEAM investigation of the structural stability and theoretical strength of Fe crystals under uniaxial loading

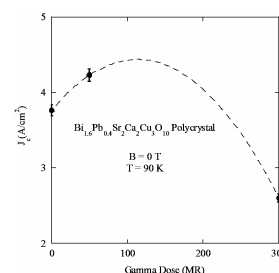
The structural stability and theoretical strength of BCC crystal Fe under uniaxial loading have been investigated with the modified analytic embedded-atom method (MAEAM). Even if an orthorhombic path is applied, the deformation is spontaneous along the tetragonal path till Milstein modified Born criterion $B_{22}-B_{23}>0$ is violated at $\lambda_1=0.9064$ in the compressive region. The branched orthogonal path with lower ...



Page 837–844 _____ I. M. Obaidat, H. P. Goeckner, B. A. Albiss, and J. S. Kouvel

Point and extended defects in superconductors

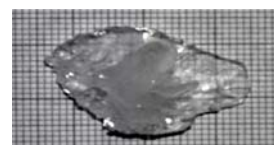
The effect of point defects created by γ -irradiation and extended defects created by Pb-ion irradiation on the behavior of the critical current density, J_c in several superconductors have been investigated. We have found a limitation of the role of both types of defects on enhancing J_c . We report an explanation of the effect of γ -irradiation and Pb-ion irradiation doses on J_c in these materials. The explanation is based on ...



Page 845–850 _____ S. Krishnan, C. Justin Raj, S. M. Navis Priya, R. Robert, S. Dinakaran, and S. Jerome Das

Optical and dielectric studies on succinic acid single crystals

Single crystals of ferroelectric succinic acid (SA) with very high degree of transparency were grown from aqueous solution by slow evaporation technique. Single crystal X-ray diffraction analysis reveals that the crystal belongs to monoclinic system with the space group $P2_1/c$. Some physical parameters have been determined for grown crystal. The optical absorption study reveals the transparency of the crystal in the entire visible region and the cut off wave length was found to be ...



Page 851–856 _____ D. Kalaiselvi, R. Mohan Kumar, and R. Jayavel

Single crystal growth and properties of semiorganic nonlinear optical L-arginine hydrochloride monohydrate crystals

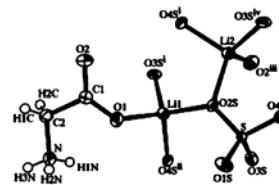
L-arginine hydrochloride monohydrate (LAHCl.H₂O) has been synthesized and single crystals have been grown from its aqueous solution by slow evaporation and slow cooling methods. The solubility of the material was measured at various temperatures and bulk crystals of size 26x13x11 mm³ have been ...



Page **857–862** _____ P. N. Selvakumar, B. Natarajan, P. Sambasiva Rao, and P. Subramanian

EPR studies of Cu(II) doped glycine lithium sulphate single crystals - a case of low hyperfine coupling constant

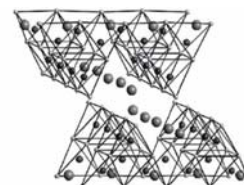
In order to rationalize the low hyperfine value for the parallel component of copper nucleus, another system with lithium as host has been investigated using Electron Paramagnetic Resonance (EPR) technique. Single crystal EPR studies have been carried out at 300 K on Cu(II) doped glycine lithium sulphate system. Angular variation of hyperfine structure lines in the three ...



Page **863–868** _____ M. Acikgoz, S. Kazan, F. A. Mikailov, E. Kerimova, and B. Aktas

Low temperature EPR spectra of Fe³⁺ centers in ternary layered TiGaS₂ crystal

The results of low temperature electron paramagnetic resonance (EPR) study of Fe doped TiGaS₂ single crystal in the temperature range of 5-300 K are presented. Iron was added to the growth mixture in amounts corresponding to a molar ratio Fe/Ga of about 1%. The EPR signal due to Fe³⁺ centers located at ...



Page **869–873** _____ S. A. Martin Britto Dhas and S. Natarajan

Growth and characterization of a new potential second harmonic generation material from the amino acid family: L-Valinium picrate

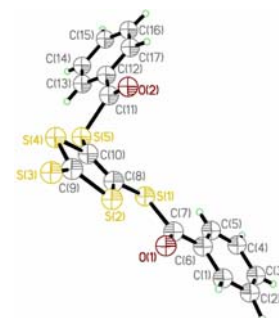
L-Valinium picrate (C₅H₁₂NO₂)⁺ · (C₆H₂N₃O₇)⁻, a non-linear optical material from the amino acid family which has large second harmonic generation (SHG) efficiency, was grown by slow evaporation method. Characterization of the crystals was made using single crystal X-ray diffraction. The functional groups and ...



Page **874–881** _____ Xinqiang Wang, Dong Xu, Guanghui Zhang, Quan Ren, and Weiliang Liu

Crystal growth, morphology, spectrographic characterization and thermal properties of 4,5-bis(benzoylthio)-1,3-dithiole-2-thione

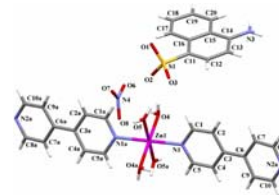
Single crystals of 4,5-bis(benzoylthio)-1,3-dithiole-2-thione (BBDT), were grown from methylene chloride and the growth morphology was deduced by the Bravais–Friedel Donnay–Harker (BFDH) model. The grown crystals were characterized by optical absorption, infrared, Raman and X-ray powder diffraction spectroscopy. The thermal behavior of BBDT has been investigated by means of thermogravimetric analysis and differential thermal analysis measurements in air.



Page **882–887** _____ Min-Le Han, Li-Wei Mi, and Wei-Hua Chen

Synthesis and crystal structure of two zinc inclusion complexes

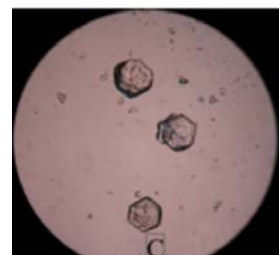
X-ray single crystals of these two inclusion complexes, $[\text{Zn}(\text{H}_2\text{O})_4\text{L}_2] \cdot (\text{4-amino-1-naphthalene sulfonate})_2$ ($\text{L} = 1,3\text{-bis(4-pyridyl) propane}$), **1**, and $[\text{Zn}(\text{H}_2\text{O})(\text{bipy})_2] \cdot (\text{4-amino-1-naphthalene sulfonate})(\text{NO}_3)$ ($\text{bipy} = 4,4'\text{-bipyridine}$), **2** were achieved by the reaction of $\text{Zn}(\text{NO}_3)_2$ and 4-amino-1-naphthalene sulfonate to 1,3-bis(4-pyridyl) propane and 4,4'-bipyridine, respectively. As inclusion complexes, the cationic components ...



Page **888–893** _____ Ji-Cheng Yin, Jin-Song Zhou, Jing Sun, Yi Qiu, Dong-Zhi Wei, and Ya-Ling Shen

Study of the crystal shape and its influence on the anti-tumor activity of tumor necrosis factor-related apoptosis-inducing ligand (Apo2L/TRAIL)

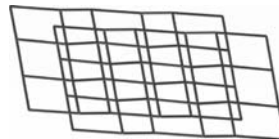
This paper describes a method about the crystal shape control improving the anti-tumor activity of tumor necrosis factor-related apoptosis-inducing ligand (Apo2L/TRAIL) in a batch cooling suspension crystallization by selecting pH values as a controllable variable. Three shaped TRAIL crystals could be obtained under different pH conditions, among which the hexagonal plate crystals had the highest specific activities against tumor cell line. The relationship ...



Page **894–898** _____ Shengwen Wang

Syntheses and crystal structures of two new coordination polymers constructed from 2-bromo-1,4-benzenedicarboxylate

To explore the possibility of obtaining the metal-organic frameworks (MOFs) bearing the 2-bromo-1,4-benzenedicarboxylate ligand, one new Mn(II) and one Co(II) coordination polymers, $[\text{Mn}(\text{HL})_2(\text{bipy})_2 \cdot 2\text{H}_2\text{O}] \cdot \text{bipy}$ (**1**) and $[\text{Co}(\text{L})(\text{bpe})]$ (**2**) ($\text{bipy} = 4,4'\text{-bipyridine}$; $\text{bpe} = 1,2\text{-bis(4-pyridyl)ethene}$) were synthesized and characterized by ...



Crystal Research and Technology is indexed in Cambridge Scientific Abstracts, CCR Database, Chemical Abstracts Service/SciFinder, ChemInform, Chemistry Citation Index™, Chemistry Server Reaction Center, Chimica Database, COMPENDEX, CSA Technology Research Database, Current Contents®/Physical, Chemical & Earth Sciences, FIZ Karlsruhe Databases, INSPEC, Journal Citation Reports/Science Edition, Materials Science Citation Index®, Reaction Citation Index™, Science Citation Index Expanded™, Science Citation Index®, SCOPUS, VINITI, Web of Science®